SOIL-CUTTING PERFORMANCE ANALYSIS OF A HANDHELD TILLER'S ROTAVATOR BY FINITE ELEMENT METHOD (FEM)

/

基于有限元法的微耕机旋耕刀辊土壤切削性能分析

Prof. Ph.D. Mingjin Yang[1, 2)], Ms. Student Po Niu[1)], Ms. Bin Peng[1)], Ph.D. Ling Yang[1)], Ph.D. Yunwu Li[1)], Prof. Xiaobing Chen[2)], Prof. Zhuomin Peng[*2)]

[1)]College of Engineering & Technology, Southwest University, Chongqing / P. R. China

[2)]Agricultural Machinery Quality Control and Inspection Technology Centre, Nanjing Research Institute for Agricultural Mechanization Ministry of Agriculture, Nanjing / P. R. China

Tel: +8615366093016; Email: zhuominp@sina.com

Abstract: *Handheld tillers are the main tilling machinery in hilly areas, with rotavators as the main tilling parts of the machines. The soil move, soil-cutting force and power consumption, accompanying the tilling process, are crucial to the performance of a handheld tiller. In this study, rotavators were chosen as a case study, and soil-cutting model of the rotavators was built and solved, by Finite Element Method (FEM), for the soil-cutting performance analysis, and the effectiveness of the analysis was validated as well, which will benefit and provide reference for design, optimization, and performance match of the handheld tillers. The results showed that: 1) during tilling process, particles of the top layer soil get the highest velocity and acceleration, and velocity and acceleration of middle layer and bottom layer particles decrease sequentially; 2) soil-cutting force of the rotavators increases to a maximum, and it gradually decreases to reach a relatively stable status with a certain fluctuation; 3) power consumption, combination of kinetic power and internal power, is mainly consumed by means of internal energy, and the ratio of kinetic power and internal power is 1: 9.5.*

Keywords: *soil-cutting, handheld tiller, rotavator, power consumption, FEM*

INTRODUCTION

Handheld tillers are the main tilling machinery in hilly areas, and the tilling land includes upland field, paddy field, blocks in greenhouse, orchards, etc. Different from traditional power tiller with power take-off from tractor to drive the machine, a handheld tiller is often driven forward by the resultant force from soil-cutting [7, 9,13]. Rotavator, as a combination of rotary blades and wheel axle, is the main tilling part of a handheld tiller. The wheel axle of the rotavator bears resultant force from rotary blade soil-cutting and driven torque from transmission, which results in complex deformations, such as bending, torsion and shearing, and strong vibration to the tiller. Therefore, structure and parameters of a rotavator directly affect the performance of a handheld tiller and have a great impact on soil-cutting quality, power consumption and balancing characteristics of the machine [6].

Since the 1990s, growing concerns about tilling issues of handheld tillers have been shown, and the implementation of Finite Element Method (FEM) and optimization has been applied more and more to the soil-cutting study. In such applications, Abo-Elnor (2003) studied the soil-tool interaction to investigate the effect of cutting speed and angle on cutting forces over large blade displacements based on predefined failure surfaces [1]. Zhou (2009) studied the stress distribution of soil and

摘要：*微耕机是丘陵山区主要的耕作机械，旋耕刀辊是微耕机的主要耕作部件。土壤切削过程中的土壤运动、切削力和消耗功率对微耕机的性能有着至关重要的影响。为了获得微耕机旋耕刀棍的土壤切削性能，本研究以旋耕刀辊为主要研究对象，通过有限元的方法，建立旋耕刀辊土壤切削模型并求解，并验证了土壤切削性能分析的有效性，为旋耕弯刀的设计、优化及微耕机的性能匹配提供参考。结果表明：1）在工作过程中，表层粒子获得的速度和加速度最大，中层粒子次之，深层粒子最小；2）旋耕刀棍土壤切削力增大到最大值后逐渐减小并在一定范围内波动；3）微耕机的功率消耗由动能和内能两部分组成，主要由内能决定，且动能、内能消耗功率比为 1：9.5*

关键词：*土壤切削；微耕机；旋耕刀辊；功率消耗；有限元*

引言

微耕机是丘陵山区的主要耕作机械，主要用于旱田、水田及温室大棚和果园等小面积作业。与传统耕耘机械动力来自拖拉机机械不同的是，微耕机前进的动力主要来自土壤的切削反力 [7，9，13]。旋耕刀辊由刀轴和旋耕弯刀组成，是微耕机的主要耕作部件。在微耕机的耕作过程中，刀轴受旋耕弯刀土壤切削过程的土壤反力和发动机驱动力矩的共同作用会发生弯曲、扭转或者剪切等复杂变形，给微耕机带来强烈振动。因而，旋耕刀辊的结构和参数直接影响微耕机的性能，对土壤切削质量、微耕机的功率消耗和平衡性等指标有较大影响 [6]。

自 20 世纪 90 年代以来，微耕机耕作问题得到了越来越多的关注。有限元法和优化越来越广泛地应用于土壤切削的研究。Abo-Elnor 研究了土壤和刀具之间的相互作用，以获悉刀具预定义疲劳表面上在大位移条件下切削速度和切削角对切削力的影响 [1]。周明等运用有有限元分析方法对

transverse knife on helical rotavator of a tiller by FEM method, and found that increased cutting speed and angle could make larger cutting resistance, between which the relationship were non-linear [12]. Xia (2013) analyzed the effects of soil-cutting parameters on tilling performance of the helical rotavator, and located the maximum equivalent stress point on the transverse knife [8]. Asl (2010) determined the mathematical model of power requirement of the rotary blades and the equations of surface area per unit volume of soil tilled, checked the validity of the model for prediction of power requirement via experiments conducted in indoor soil bin, and obtained optimized rotary blade [2]. Yang (2014) simulated and evaluated the power consumption of a handheld tiller's rotary blade at different levels of control factors of soil-cutting parameters by method of Smoothed Particle Hydrodynamics (SPH) [10]. But, the studies mentioned above were mostly focused on the soil-blade interaction, and literatures regarding to soil-cutting performance of the rotavators of a handheld tiller can scarcely be found. Then, references for design, optimization, and performance match of the handheld tillers are not enough to rely upon.

In this study, rotavators of a handheld tiller were chosen as a case study, and the soil-cutting model of the rotavators was built and solved by FEM Method within ANSYS for the soil-cutting performance analysis, and the effectiveness of the analysis was validated as well.

MATERIAL AND METHOD

Material

Considering the climate, geological conditions and soil characteristics in Chongqing, China, soil model MAT147 by LS-DYNA was adopted in this study [3,16]. Parameters of soil were defined for FEM analysis, as shown in Table 1.

Rotary blades (rotary radius 185mm) of type III suitable for shallow tillage were employed. The blades were qualified for Chinese national standard GB/T 5669-2008 [14]. Parameters of the blades were defined, as shown in Table 2.

Method

a) FEM model of soil-cutting

Main links to set up a FEM model of soil-cutting of a rotavator are as follows:

1) FEM model of rotavator

Build the 3-D solid model of the rotavator by Pro/E, as

土壤剪切力的分布和螺旋型旋耕刀辊横刀工作机理进行了研究，指出直线型横刀切削阻力随着切削速度和切削角度的增大而增大并呈非线性关系 [12]。夏俊芳研究了土壤切削参数对螺旋刀辊的耕作性能的影响，确定了螺旋横刀最大等效应力发生部位 [8]。Asl 确定了旋耕弯刀功率消耗的数学模型和单位面积切土量的方程，校验了通过数学模型预测的功率消耗和室内土槽实验结果，并得到优化的旋耕弯刀 [2]。杨玲基于光滑粒子流体动力学方法 SPH 的方法模拟和评价了不同土壤切削参数和因子水平条件下的微耕机旋耕弯刀的功率消耗[10]。但是上述研究大多集中在旋耕弯刀和土壤的相互作用，关于微耕机旋耕刀辊土壤切削性能相关的研究文献很难发现，因而不足以为微耕机设计、优化和性能匹配提供足够的参考和支撑。

本研究以微耕机旋耕刀辊为主要研究对象，通过 ANSYS 建立微耕机旋耕刀辊土壤切削有限元模型并求解，分析了旋耕刀辊土壤切削性能，同时对分析的有效性进行了校验。

材料和方法

材料

结合中国重庆地区气候、地质条件以及土壤特性，本研究采用 LS-DYNA 中提供的 MAT147 土壤模型 [3，16]。确定用于有限元分析的土壤的具体参数，见表 1。

采用 III 型旋耕弯刀，该型弯刀适于浅耕作业，回转半径 185mm。旋耕弯刀符合中国国家标准 GB/T 5669-2008 相关规定 [14]。旋耕弯刀的参数见表 2。

Table 1

Parameters of soil

Parameters	Value
Bulk density, kg/mm^3	2.35e-6
Porosity, %	39.2
Specific gravity	2.68
Bulk modulus, Pa	3.5e+07
Moisture, %	21
Shear modulus, Pa	2.0e+07
Within friction angle, radian	0.436
Cohesion, Pa	2.2e+04

Table 2

Parameters of rotary blade

Parameters	Value
Rotary radius, mm	185
Material	65Mn
Density, kg/mm^3	7.83e+3
Elastics modulus, Pa	2.07e+11
Poisson's ratio	0.35

方法

a）旋耕刀辊土壤切削有限元模型

建立旋耕刀辊土壤切削有限元模型的主要步骤为：

1）旋耕刀辊有限元模型的建立

通过 Pro/E 建立旋耕刀辊的 3-D 实体模型，如图 1 所示。

shown in Figure 1, and save it as format .igs or .*x-t. Import the model to HyperMesh to mesh grids with grid size 6mm, and refine them according to requirement of surface complexity of the rotavator, then the FEM model of the rotavator was obtained, as shown in Figure 2.

将建立好的实体模型以.igs 或.*x-t 格式保存，导入 HyperMesh 中，定义网格尺寸为 6mm 并进行网格划分，由于旋耕刀辊曲面复杂，根据要求对网格进行细化，网格细化后得到旋耕刀辊的有限元模型，如图 2 所示。

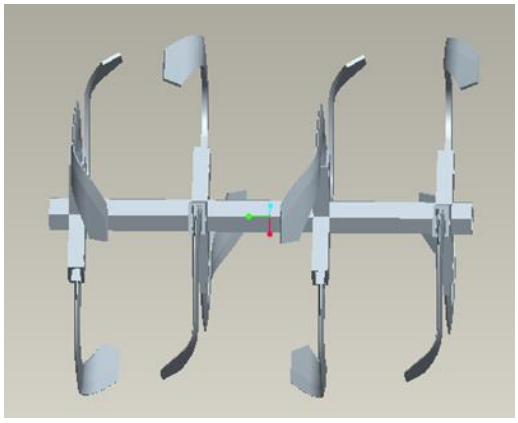

Fig.1 - The 3-D solid model of rotavator

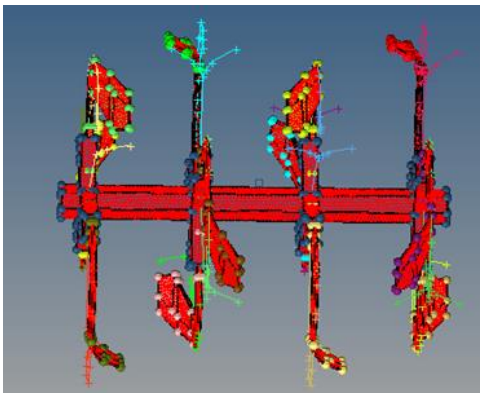

Fig.2 – The FEM model of rotavator

2) FEM model of soil

According to soil model MAT147 provided by ANSYS, build the 3-D solid model of soil with dimensions as required. Transform the solid model to SPH model in LS-PREPOST, and define element types and parameters of the soil. Set Lagrange single-point integration algorithm, and mesh grids with grid size of 10mm, then the FEM model of soil (soil SPH model) was obtained, as shown in Figure 3.

2）土壤有限元模型

根据 ANSYS 提供的 MAT147 土壤模型和实际土壤尺寸，建立土壤 3-D 实体模型。在 LS-PREPOST 内将土壤实体模型转化为 SPH 模型，定义单元类型和土壤材料，采用 Lagrange 型单点积分算法，定义网格尺寸为 10mm，并对模型进行进行划分，建立土壤有限元模型（土壤 SPH 模型），如图 3 所示。

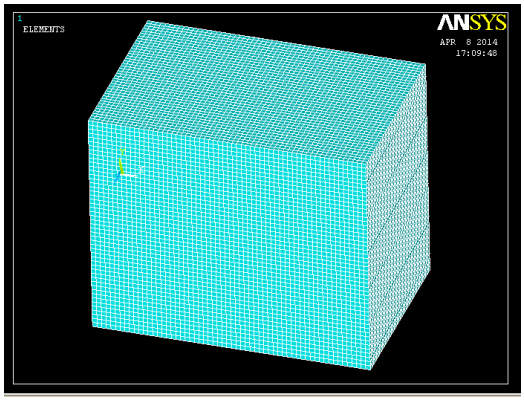

Fig.3 - The FEM model of soil

3) Boundary condition and contact

Define rotary blades of the rotavator as rigid bodies with stable forward speed and rotation speed, and add symmetry constraint SPH_SYMMETRY_PLANE for the soil SPH model on both sides and bottom surfaces of the soil. Define rotary blades as contact PART and soil as target PART, and add the contact between rotary blades and the soil as AUTOMATIC_NODES_TO_SURFACE. Set sliding interface penalties 0.2, and dynamic and static coefficient friction 0.20, 0.18, respectively [9].

4) FEM model of soil-cutting

Import the FEM model of rotavator to LS-PREPOST, generate SPH (soil SPH model) for the rotavator, and load parameters of the rotavator and soil-cutting on Keyword Manager panel in LS-PREPOST, then the FEM model of soil-cutting was available for process, as shown in Figure 4.

3）边界条件及接触

定义旋耕刀辊的旋耕弯刀为刚体，旋耕弯刀前进速度和回转速度稳定。对土壤 SPH 模型添加对称约束 SPH_SYMMETRY_PLANE，约束土壤两侧面和底面。定义旋耕弯刀为接触 PART，土壤为目标 PART。添加旋耕弯刀与土壤之间的接触为自动点面接触 AUTOMATIC_NODES_TO_ SURFACE。设定滑动界面惩罚因子为 0.2，动、静摩擦因子分别为 0.18 和 0.20 [9]。

4）旋耕刀辊土壤切削有限元模型的建立

将旋耕刀辊有限元模型导入 LS-PREPOST 中，为旋耕刀辊生成土壤 SPH 模型，在 LS-PREPOST 的 Keyword 管理界面添加旋耕刀辊和土壤切削参数，从而得到旋耕刀辊土壤切削有限元模型，如图 4 所示。

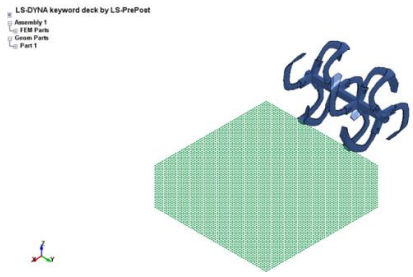

Fig.4 - The FEM model of soil-cutting

b) Power consumption of soil-cutting

The power consumption of soil-cutting of a rotavator consists of 2 parts, and one is for the machine moving forward, and the other is for the soil-cutting and soil-throwing. Define the former as kinetic power, and the latter as internal power, and the power consumption can be calculated by empirical method as follows:

1) Kinetic power

The kinetic power for the handheld tiller moving forward can be expressed as [4]:

b）微耕机刀辊土壤切削功率消耗

旋耕刀辊土壤切削的功率消耗由用于旋耕刀辊前进的动能功率消耗和用于土壤变形和运动的内能功率消耗两部分组成，其功率计算公式分别如下。

1）动能功率

旋耕刀辊前进消耗的动能功率可由下式计算 [4]：

$$P = Fv_m \quad (1)$$

Where, P is kinetic power kW; F is the resultant force along the forward move of the tiller, N; v_m is the forward speed of the tiller, m/s.

2) Internal power

The internal power can be expressed as follow [15]:

式中，P 为旋耕刀辊前进的动能功率，kW；F 为微耕机沿前进方向的土壤反力，N；v_m 为微耕机的前进速度，m/s。

2）内能功率

用于土壤变形和运动的内能功率可由下式计算[15]：

$$N = 0.1K_\lambda dv_m B \quad (2)$$

where N is internal power, kW; K_λ is tillage resistance of rotary tilling, N/cm^2, and $K_\lambda = K_1K_2K_3K_4K_n$; K_n is soil resistance, and $K_n = 12$ for common clay soil, with stubble, of moisture content 20% and tilling depth 13cm. K_1 is correction coefficient for tilling depth, K_2 is correction coefficient for moisture content of the soil, K_3 is correction coefficient for vegetation conditions of the soil, and K_4 is the correction coefficient for operation mode of the tilling operation. Set $K_1 = 0.93$, $K_2 = 1.0$, $K_3 = 1.1$, and $K_4 = 0.71$ in this study. d is tilling depth, cm; B is tilling width, m.

式中，N 为刀辊土壤切削和抛土功耗，kW；K_λ 为旋耕比阻，N/cm^2，$K_\lambda = K_1K_2K_3K_4K_g$；$K_g$ 为土壤阻力系数，对于一般粘土、麦茬，耕深 13cm，土壤含水率为 20%，土壤阻力系数一般取 13；K_1 为耕深修正系数，取 1.0；K_2 为土壤含水率修正系数，取 0.93；K_3 为植被修正系数，取 1.1；K_4 为作业方式修正系数，取 0.71；d 为耕深，cm；B 为耕作幅宽，m。

RESULTS

By solving the FEM model of soil-cutting of the rotavator, the information of soil move with animation effect, soil-cutting force, and power consumption can be obtained for the corresponding analysis.

Soil move

From the animation information of soil move while soil-cutting of the rotavator, the following findings were observed: during the soil-cutting, there is no soil move before rotary blades contact the soil. With rotavator travelling forward, the lengthwise edges of two blades on the rotavator firstly contact the soil concurrently, and the soil is cut apart by the blades along forward direction. With the rotavator travelling further, the contact areas and contact points between soil and blades increase, and the soil particles, surrounding the blades, are driven apart along surfaces of the rotary blades under the co-act of shearing and squeezing, which results in the soil deformation and move. Then, the particles move with parabolic mode after they leave the surface of rotary blades to obtain effects of soil-throwing and pulverization.

For quantitatively studying the soil move of different tillage layers, 3 SPH soil particles, representing surface layer, middle layer, and deep layer of tillage soil, were

结果与分析

通过求解旋耕刀辊土壤切削有限元模型，可以获悉带动画效果的土壤运动情况、土壤切削力和土壤切削功率消耗等信息，并进行相关分析。

土壤运动

通过对旋耕刀辊土壤切削过程土壤运动动画分析可知：在土壤切削过程中，在旋耕弯刀接触土壤表层之前，土壤粒子没有运动变化，随着旋耕刀辊的旋转前进，两把旋耕弯刀的侧切刃同时首先接触土壤，在旋耕弯刀的作用下，土壤沿弯刀前进方向被切割分开，随着刀辊的继续前进，弯刀与土壤的接触面积增大，接触点增多，刀片周围的土壤粒子在弯刀剪切和挤压的作用下沿刀片表面散开，使土壤发生变形和运动。土壤粒子以抛物线的模式运动离开旋耕弯刀表面，从而获得抛土和碎土的效果。

为了定量研究不同耕层土壤的运动情况，在 SPH 粒子中选取 3 个粒子分别代表土壤表层粒子 28885（A）、中层粒子 30000（B）和深层粒子 29992（C）以进行土壤运动分

chosen for soil move analysis, and they were numbered as 28885 (A), 30000 (B), and 29992 (C), in Fig.5.

析，土壤粒子标记如图 5 所示。

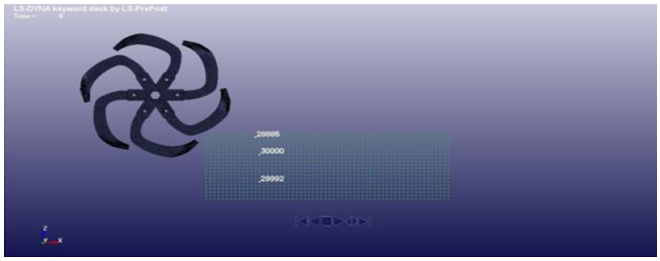

Fig.5 - Marked SPH soil particles

By solving the FEM model of soil-cutting of the rotavator, the velocity, acceleration and displacement curves of the particles were obtained by means of simulation, as shown in Figure 6. Of which, the red curves were of particle A, green curves were of particle B, and blue curves were of particle C. From curves of velocity and acceleration of the marked SPH soil particles as shown in Figures 6 a) and 6 b), there are 3 stages of the particles' move: 1) during 0-0.3s, the rotary blades of the rotavator does not contact the 3 marked soil particles, and the particles does not show any obvious move with small values of velocity and acceleration; 2) during 0.3-0.8s, the rotary blades start to contact the marked particles, and the particles of different layers, subjected to forces from rotary blades and the surrounding soil, obtain different velocity and acceleration as: particles of the top layer particles get the highest velocity and acceleration, and velocity and acceleration of middle layer and bottom layer particles decrease sequentially; 3) after 0.8s, the rotary blades leave the marked particles, and the forces acting on the particles decrease, then the velocity and acceleration decrease as well. Furthermore, from curves of displacement of the marked SPH soil particles as shown in Figure 6 c), after the contact of soil and blades, the top layer particles get the highest displacement, which reflects that the top layer soil is deformed and destroyed seriously because of shearing force provided by the rotary blades of the rotavator. This soil move observation has a similar pattern as Xia's study [8]

通过求解旋耕刀辊土壤切削有限元模型和仿真分析，可以获悉不同深度粒子速度曲线、加速度曲线和位移曲线，如图 6 所示。其中，粒子 A 用红色线条表示，粒子 B 用绿色线条表示，粒子 C 用蓝色线条表示。通过对图 6 a）、6 b）的速度曲线和加速度曲线分析可得，粒子的运动有 3 个过程：1）在 0-0.3s 阶段，刀辊的旋耕弯刀没有切削到标记的 SPH 粒子时，3 个粒子几乎都没有运动变化，其速度和加速度值很小；2）0.3-0.8s 阶段，旋耕弯刀开始接触到标记粒子，不同耕层土壤粒子受到旋耕弯刀和周围土壤的力的作用，获得不同的速度和加速度：表层粒子的速度和加速度最大，中层粒子次之，深层粒子的速度和加速度最小；3）在 0.8s 之后，旋耕弯刀离开标记粒子，土壤粒子受力减小，速度和加速度也同时减小。而且，通过对图 6 c）中标记 SPH 土壤粒子的位移曲线可知：经历旋耕弯刀和土壤的接触以后，表层土壤粒子的位移量最大，这表明表层土壤粒子由于旋耕刀辊弯刀提供的剪切力而产生的变形和破坏严重。这种土壤运动现象与夏俊芳研究得到的土壤运动方式相似 [8]。

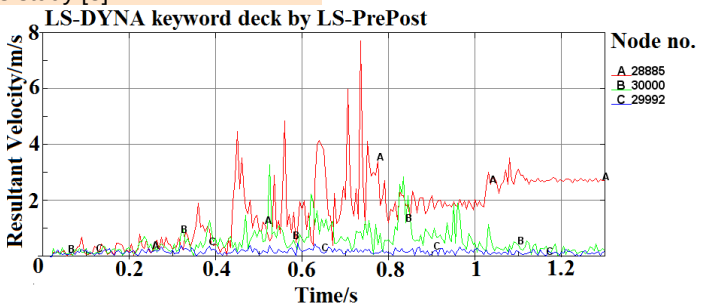

a)

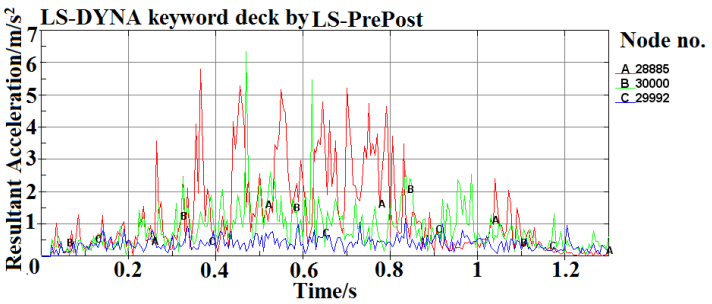

b)

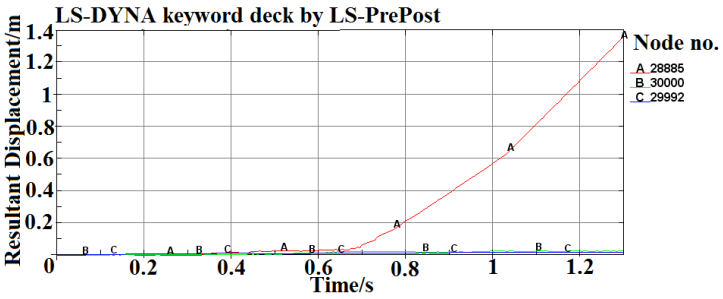

c)

Fig.6 - Soil move of different layers
a) Speed curve; b) Acceleration curve; c) Displacement curve

Soil-cutting force

The curve of soil-cutting force by FEM method was obtained, as shown in Figure 7. In the initial stage of soil-cutting, the soil-cutting force is relatively small with low fluctuations, and with the processing of soil-cutting, the soil-cutting force increases gradually, and it reaches a certain status with a relatively high fluctuations. The reason for the observed curve pattern of soil-cutting force is as follows: in the initial stage of soil-cutting, there are only two rotary blades on the rotavator contact the soil, and after that more and more blades take part in the soil-cutting operation to stabilize the soil-cutting force. This soil-cutting force observation coincides with Lin's study on that of rotary blade [5].

In fact, when the rotary blades start to contact the soil, with the forward travel of the blades, the contact areas of soil-blade increase, the soil deforms elastically, and the force acting on the soil increases gradually. With the increases of deformation and force acting on the soil, the soil deforms plastically, and it follows the soil hardening, then the soil-cutting force reaches maximum value, and the soil structure breaks down and is destroyed accordingly. After that, there is soil softening effect which results in decrease of soil-cutting force. Therefore the soil-cutting process is stabilized at a status with a certain fluctuations [12].

土壤切削力

通过有限元法得到土壤切削力曲线，如图 7 所示。在土壤切削的初始阶段，土壤切削力很小，并且在一个较小范围内波动。随着切削过程的进行，切削力逐渐增大并达到一定水平，其波动也相对较大。这种土壤切削力曲线变化主要原因在于：在土壤切削的初始阶段，旋耕刀辊只有两把旋耕弯刀接触并切削土壤，随着时间增加，均匀布置的多把旋耕弯刀依次切削土壤，使切削力变得均匀稳定。这种土壤切削力的现象与林昌华对旋耕弯刀的研究结论吻合 [5]。

事实上，当旋耕弯刀开始接触土壤，随着旋耕弯刀不断前行，刀具和土壤的接触面积增大，土壤产生弹性变形，作用在土壤上的切削力逐渐增加。随着土壤变形和土壤切削力的增加，土壤产生塑性变形，随之产生土壤硬化，此时土壤切削力达到最大值，土壤结构遭到破坏，发生初始失效，土壤切削力逐渐减小。因而土壤切削过程进入稳定切削状态，但土壤切削力在一定范围内波动 [12]。

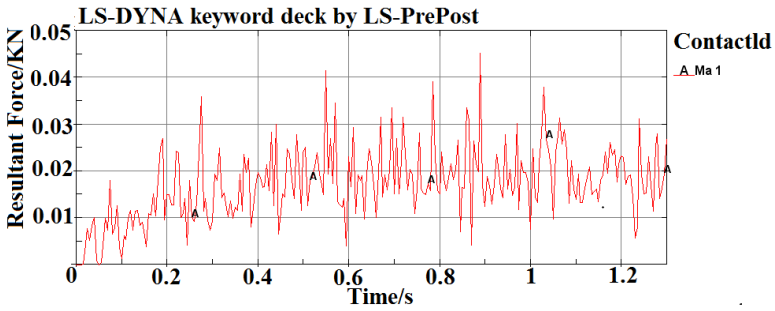

Fig.7 - Soil-cutting force

Power consumption

The curves of energy of soil-cutting by FEM method were obtained, as shown in Figure 8. Of which, Figure 8 (a) is curve of kinetic energy, Figure 8 (b) is curve of internal energy, and Figure 8 (c) is curve of total energy of soil-cutting, and the energy information can be employed to calculated the corresponding power consumption. The total energy of soil-cutting is the addition of kinetic energy and internal energy. The total energy of soil-cutting of rotavator increases linearly after the initial soil-cutting stage. The internal energy constitutes a high proportion of total energy of soil-cutting, namely, the power consumption of soil-cutting is mainly consumed by means

功率消耗

通过有限元法得到土壤切削能量曲线，如图 8 所示。其中，土壤切削过程的动能消耗如图 8 a）所示，内能消耗如图 8 b）所示，总能量消耗如图 8 c）所示。土壤切削能量信息可以用于计算相应的土壤切削功率消耗。土壤切削总能量消耗是内能消耗和动能消耗之和。在经历了土壤切削初始阶段以后，旋耕刀辊土壤切削力线性增加。内能组成了土壤切削总能量的大部分，也就是说，土壤切削功率主

of internal energy. According to power consumption Equations (1) and (2) in section 2, taking a handheld tiller SR1Z-80 with mass 80kg and rated power 4kW (manufactured by Chongqing Shineray Agricultural Machinery Co., Ltd.) as an example, the power consumption by means of kinetic energy and internal energy was 0.15kW and 1.42kW for one rotavator of the tiller (the handheld tiller brings 2 rotavators for the tillage), and the ratio of kinetic energy and internal energy is 1:9.5, and it is consistent with the relationship between curves of kinetic energy and internal energy of soil-cutting as shown in Figure 8, which validates effectiveness of the FEM analysis of soil-cutting.

要通过内能的方式消耗。根据公式（1）和（2），以重庆鑫源农机股份有限公司生产的 SR1Z-80 微耕机（80kg，4kW）为例。微耕机一个旋耕刀辊通过动能和内能消耗的功率分别为 0.15kW 和 1.42kW（一台微耕机带左右 2 个旋耕刀辊），动能和内能消耗的功率之比为 1：9.5，这与图 8 中土壤切削动能和内能曲线关系相符合，验证了旋耕刀辊土壤切削有限元分析的有效性.

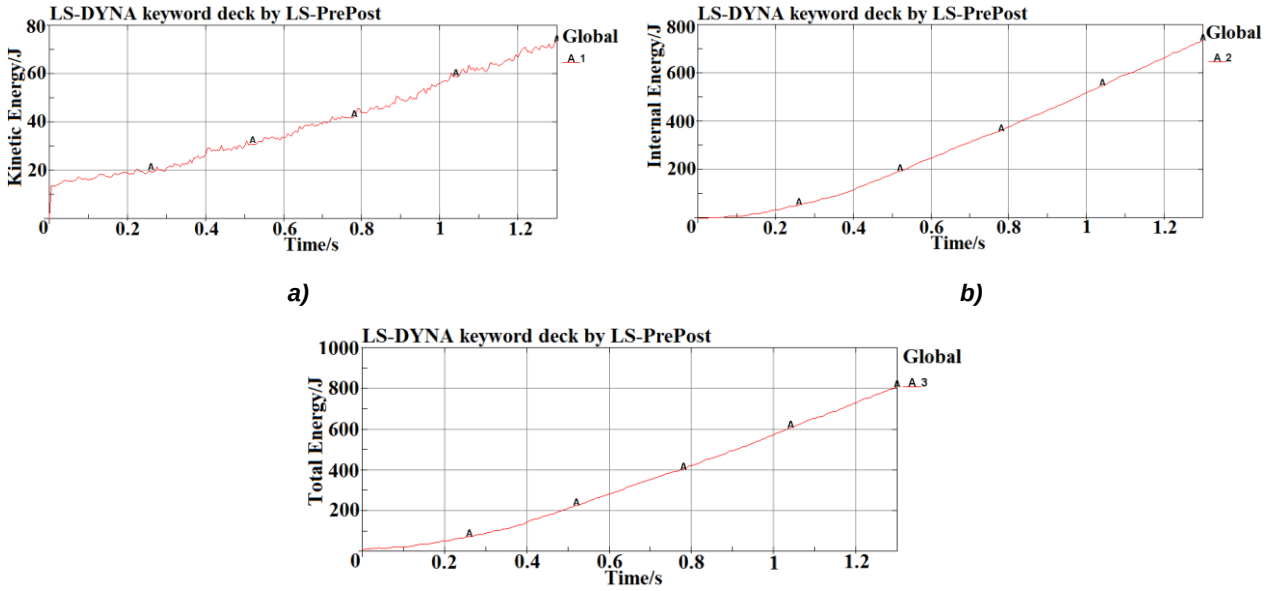

Fig.8 - Total energy of soil-cutting
a) Kinetic energy; b) Internal energy; c) Total energy

CONCLUSIONS

The soil-cutting performance analysis of a handheld tiller's rotavator by FEM method was conducted, and the effectiveness of the analysis was validated in this study. During soil-cutting of the rotavator, soil of different layers gets different velocity and acceleration, and the top layer soil gets the highest velocity and acceleration. The soil-cutting force increases to a maximum, and follows a gradual decrease to reach a relatively stable status with some fluctuation. Power consumption, combination of kinetic power and internal power, is mainly consumed by means of internal energy, with ratio of kinetic power and internal power 1: 9.5.

ACKNOWLEDGEMENT

The study was supported by the National Natural Science Foundation of China (No. 51475385), the Scientific Research Foundation for the Returned Overseas Chinese Scholars, Ministry of Education of China (No. 2013-1792), Fundamental Research Funds for the Central Universities of China (No. XDJK2014C033), and Funds from Nanjing Research Institute for Agricultural Mechanization, Ministry of Agriculture (2014-1053).

REFERENCES

[1]. Abo-Elnor M., Hamilton R., Boyle J.T., (2003) - *3D dynamic analysis of soil-tool interaction using the finite element method.* Journal of Terramechanics, vol. 40, no. 1/2003, ISSN 0022-4898, pg. 51-62;

结论

通过有限元法分析了微耕机旋耕刀辊的土壤切削性能，验证了土壤切削性能分析的有效性。在旋耕刀辊土壤切削过程，不同深度的粒子获得不同的速度和加速度，表层粒子获得的速度和加速度最大。土壤切削力先增加到最大值，之后逐渐减小从而进入稳定切削状态，并在一定范围内波动。功率消耗，主要包括动能功率消耗和内能功率消耗，且主要由内能功率消耗决定，动能功率消耗和内能功率消耗之比为 1：9.5。

致谢

本研究得到中国国家自然科学基金项目（51475382）、中国教育部留学回国人员科研启动基金（2013-1792）、中国中央高校基本科研业务费专项资金资助项目（XDJK2014C033）和中国农业部南京农机化研究所资助项目（2014-1053）的资助。

参考文献

[1] Abo-Elnor M., Hamilton R., Boyle J. T. (2003) - *3D dynamic analysis of soil-tool interaction using the finite element method*. Journal of Terramechanics, 第 40 卷，第 1 期/2003, ISSN 0022-4898, 51-62;

[2]. Asl J.H., Surendra S., (2009) - *Optimization and evaluation of rotary tiller blades: computer solution of mathematical relations.* Soil and Tillage Research, vol.106, no. 1/ 2009, ISSN 0167-1987, pg. 1-7;
[3]. Lewis B.A., (2004) - *Manual for LS-DYNA soil material model 147.* Report of Turner-Fairbank Highway Research Center, Georgetown, USA;
[4]. Li B., (2008) - *Agricultural machines,* China Agriculture Press, ISBN 978-7-109-08403-2, Beijing, P. R. China;
[5]. Lin C., Kang S., Qin F., et al., (2015) - *Simulation analysis and optimization of rotary blade on FEM.* Agricultural Development & Equipments, no. 1/2015, ISSN 1673-9205, pg. 55-57;
[6]. Peng B., (2014) - *Modeling and simulation of soil-cutting dynamics of rotary roller of mini-tiller.* M.S. thesis, Southwest University, P. R. China;
[7]. Shi L., Zhang H., Zhai Z., et al, (2004) - *Present situation and development of two-wheel tractor*. Journal of Agricultural Mechanization Research, no. 5/2004, ISSN 1003-188X, pg. 1-3;
[8]. Xia J., He X., Yu S., et al., (2013) - *Finite element simulation of soil cutting with rotary knife roller based on ANSYS/LS-DYNA software.* Transactions of the Chinese Society of Agricultural Engineering, vol. 29, no. 10/2013, ISSN 1002-6819, pg. 34-41;
[9]. Xue Z., Lv X., Tang W., (2011) - *The simulation of soil cutting with screw cutter based on ANSYS/LS-DYNA971.* Journal of Agricultural Mechanization Research, vol. 33, no. 4/2011, ISSN 1003-188X, pg. 13-16;
[10]. Yang L., Zhu L.-X., Chen J., et al, (2014) - *Simulation and evaluation of soil-cutting power parameter of a handheld tillers rotary blade.* International Agricultural Engineering Journal, vol. 23, no. 4/2014, ISSN 0858-2114, pg. 21-27;
[11]. Zeng D., (1995) - *Machinery-soil dynamics*, Beijing Science and Technology Press, ISBN 7-5304-1602-2, Beijing, P. R. China;
[12]. Zhou M., (2009) - *Research on FEM-based working mechanism of transverse knife on helical rotary roller.* M.S. thesis, Huazhong Agricultural University, P. R. China;
[13]. Zhu L., Yang L., Yang M., et al, (2011) - *Technical status and development trend of the mini-tiller in China.* Journal of Agricultural Mechanization Research, vol. 33, no. 7/ 2011, ISSN 1003-188X, pg. 236-239;
[14]. *** Chinese Standard Committee, (2008) - *Rotary tiller-rotary blades and blade holders*, *GB/T 5669-2008*. Chinese Standard Press, P. R. China;
[15]. *** Chinese Academy of Agricultural Mechanization Sciences, (2007) - *Design manual of agricultural machinery,* Chinese Agricultural Science and Technology Press, ISBN 978-7-80233-335-2, Beijing, P. R. China;
[16]. *** U.S. Department of Transportation Federal Highway Administration, (2004) - *Evaluation of LS-DYNA soil material model 147.* Report of Turner-Fairbank Highway Research Center, Georgetown, USA.

[2]. Asl J.H., Surendra S. (2009) - *Optimization and evaluation of rotary tiller blade: computer solution of mathematical relations*. Soil & Tillage Research. 第 106 卷, 第 1 期/2009, ISSN 0167-1987, 1-7;
[3]. Lewis B.A., (2004) - *Manual for LS-DYNA soil material model 147*. Report of Turner-Fairbank Highway Research Center, Georgetown, USA;
[4]. 李宝筏. (2008) - *农业机械学.* 中国农业出版社，ISBN 978-7-109-08403-2, 北京, 中国;
[5]. 林昌华, 康松林, 秦飞龙, 等. (2015) - *旋耕刀有限元仿真分析及优化*. 农业开发与装备, 第 1 期, ISSN 1673-9205, 55-57;
[6]. 彭彬. (2014) - *微耕机刀辊切土动力学建模及仿真*. 硕士论文, 中国: 西南大学;
[7]. 时玲, 张海东, 翟兆斌, 等. (2004) - *我国微耕机技术现状与发展方向*. 农机化研究, 第 5 期/2004, ISSN 1003-188X, 1-3;
[8]. 夏俊芳, 贺小伟, 余水生, 等. (2013) - *基于 ANSYS/LS-DYNA 的螺旋刀辊土壤切削有限元模拟*. 农业工程学报, 第 29 卷, 第 10 期/2013, ISSN 1002-6819, 34-41;
[9]. 薛子萱, 吕新民, 唐卫卫. (2011) - *螺旋刀具土壤切削过程模拟分析 - 基于ANSYS/LS-DYNA971*. 农机化研究, 第 33 卷, 第 4 期/2011, ISSN 1003-188X,13–16;
[10]. Yang L, Zhu L-X, Chen J, et al. (2014) - *Simulation and evaluation of soil-cutting power parameter of a handheld tillers rotary blade*. International Agricultural Engineering Journal, 第 23 卷, 第 4 期/2014, ISSN 0858-2114, 21-27;
[11]. 曾德超. (1995) - *机械土壤动力学*. 北京科学技术出版社, ISBN 7-5304-1602-2, 北京, 中国.
[12]. 周明. (2009) - *基于有限元法的螺旋型旋耕刀辊横刀工作机理研究*. 中国: 华中农业大学;
[13]. 朱留宪, 杨玲, 杨明金, 等. (2011) - *我国微型耕耘机的技术现状及发展*. 农机化研究, 第 33 卷, 第 7 期/2011, ISSN 1003-188X, 236-239;
[14]. 中国国家标准化管理委员会, (2008) - *旋耕机械刀和刀座, GB/T 5669-2008*. 中国标准出版社, 中国;
[15]. 中国农业机械化科学研究院. (2007) - *农业机械设计手册*. 中国农业科学技术出版社, ISBN 978-7-80233-335-2, 北京, 中国;
[16]. U.S. Department of Transportation Federal Highway Administration, (2004) - *Evaluation of LS-DYNA soil material model 147*. Report of Turner-Fairbank Highway Research Center, Georgetown, USA.